

Nonferrous Metal Sorter Final Report

The Metal People:

Tyler Shewbert

Evan Zaro

Justin Yau

Abstract

The inefficient sorting methods of nonmagnetic metals can be improved by the implementation of a nonferrous (meaning nonmagnetic) electromagnet. Scrap metal recycling companies use hand sorting or chemical density sorting for nonmagnetic metals. These methods are time and labor intensive. The Nonferrous Metal Sorter project aims to reduce the need of manual labor, use of chemicals, and the time it takes to sort these metals by creating a testbed which attracts nonmagnetic metals such as copper or aluminum by making use of a special electromagnet. This magnet, also called a nonferrous magnet, can vary its frequency with the help of a control system. The variable frequency is important, as it allows for specific nonmagnetic metals to be targeted for attraction. For example, as nonmagnetic scrap is sent down a chute or a conveyor belt, nonferrous magnets set at different frequencies will attract specific nonmagnetic metals, thus sorting the scrap. This report will discuss the initial magnet design and construction which was based on Leonard Crow's research on nonferrous metal attraction. In order to control the variable frequency required to attract different nonmagnetic metals, an inverter was built. Experimentation on the initial design led to the construction of an improved second magnet and a customized control system. This control system is the focus of our design and is the major component of our testbed. It is comprised of the inverter for frequency control, a capacitor bank for power factor correction, and a sensor network to monitor the system.

Introduction

In a 1951 paper, Leonard Crow discussed techniques that could be used to attract aluminum and copper through the use of modified electromagnets. Using his concept we wanted to develop a nonferrous metal sorter that would attract different metals at unique frequencies. The purpose for constructing such a device is to enable scrap metal recyclers to improve the efficiency of their sorting system. Currently, nonferrous metals are sorted by hand or chemical density sorting methods. Both of these are economically inefficient in terms of time, labor, and material. We have been successful in constructing a functional testbed that will allow future research to prove that attractive, nonferrous metal sorting can differentiate between metals, however, we were not able to prove this by the end of this school year. We split this project into four major milestones:

The first milestone was the development of a specialized electromagnet which was based on Crow's design. Using 60 Hz AC, the electromagnet has the ability to attract aluminum and copper. This milestone was achieved and was the major deliverable for the winter quarter.

The second milestone was modifying the power source of the magnet to operate with a DC source. This was necessary so that the magnetic field frequency of the magnet could be varied using an inverter. This component was essential in attempting to achieve the major stretch goal for this project, which was to show the magnet could attract copper and aluminum when set to different frequencies.

The third major milestone was the attachment of voltage, current and temperature sensors. These sensors are used for data collection, operation, and the protection of the magnet.

The fourth major milestone was the development of code that would use current measurements to track the mass of the material being picked up by the electromagnetic. However, it was found during our research that this was not possible since there was no relationship between current being drawn and the mass being attracted. Code was developed to operate the magnet, the sensor network, and to provide overtemperature protection. PCBs integrating the controls for the inverter and the sensors were built.

The completed design will function as a testbed for future researchers to test whether differentiated, frequency-based nonferrous metal sorting is possible and economically practical. The following block diagram shows the completed system that will function as the testbed:

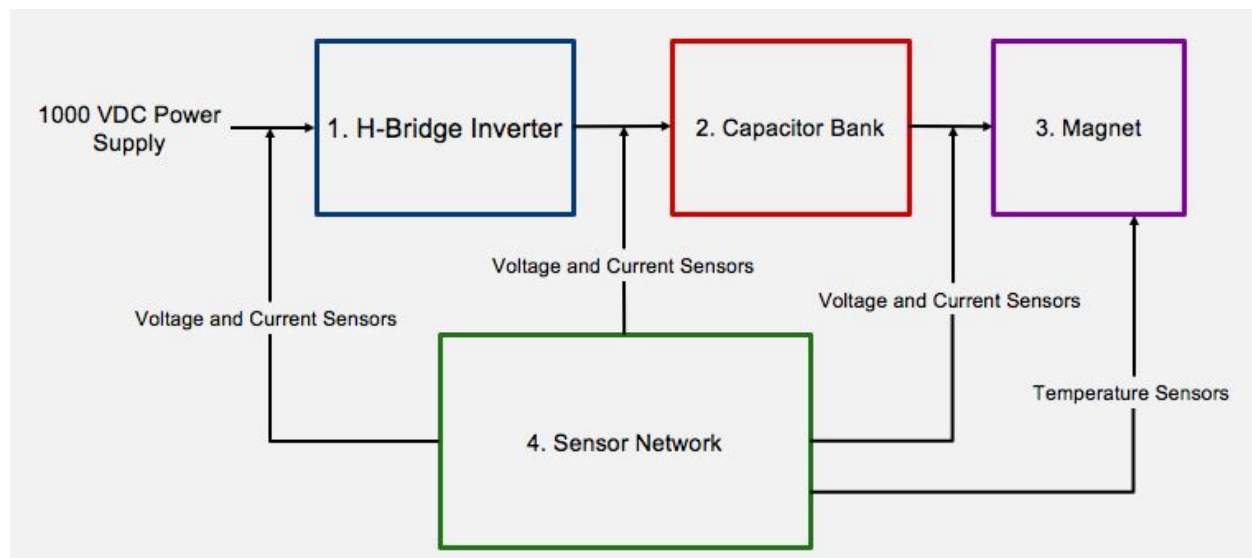


Figure 1: Systems level block diagram

The first major block of the systems diagram is the H-Bridge Inverter. The purpose of the inverter is to give control over the frequency of the magnetic field of the magnet. The inverter is comprised of four insulated gate bipolar transistors (IGBT) which are switched on and off by a digital signal processor (DSP). The DSP controls the IGBTs by using sine-triangle modulation and

was programmed using Simulink. As the diagram above depicts, the inverter is powered by a 1000 V DC supply. The inverter controls the magnet through the capacitor bank.

The impedance of the magnet changes as the frequency, controlled by the inverter, is varied. In order to compensate for this change in impedance, the capacitor bank was created. The purpose of the capacitor bank is to add power factor correction between the inverter and the magnet. The capacitor bank is comprised of seven series and six parallel 1 μF capacitors. With the use of relays, it can alter its capacitance by changing the combination of capacitors as the magnet's frequency is swept from 150 to 1000 Hz. The capacitor bank switching is controlled by the operator via a ring encoder.

In order to attract nonmagnetic test pieces, a special electromagnet with a specific geometry was created. As previously mentioned, this magnet follows Leonard Crow's design. The magnet itself is made of a laminated steel outer cylinder and inner core. A copper ring is placed around the inner core while 778 turns of 18 AWG copper wire was wrapped around the outer cylinder. This provides the appropriate geometry for the magnet to generate the appropriate field of attraction for the nonmagnetic metals.

In order to analyze the system and keep the magnet from overheating, a sensor network was created. The sensor network contains multiple voltage and currents sensors with one temperature sensor. An issue with the magnet is that it can reach component damaging temperatures, which cause the enamel of the copper wires to melt. The sensor network also connects to two LCD displays which shows important information to the operator including voltages, currents, temperature, frequency, and the value of the capacitor bank. When the temperature reaches an upper limit it will shut off the system to prevent overheating.

When designing this system, we started with the initial design and construction of the magnet. After the initial magnet was built, we constructed the inverter which then led to the construction of the second magnet. Issues with the inverter and second magnet gave rise to the need for power factor correction, leading to the creation of the capacitor bank. In order to properly analyze and control the system, we created the sensor network. All of these components then required proper casing and cooling before they were finally integrated together.

Initial Magnet Design and Construction

The nonferrous magnet operates based on the principle that diamagnetic materials induce eddy currents, which produce a magnetic field in an opposing direction when introduced to an external magnetic field. Introducing two pieces of diamagnetic materials into a magnetic field will

induce repulsive forces on each piece; this means that each object will create a magnetic field in the same opposing direction to the external magnetic field. While the diamagnetic objects are being repelled by the external magnetic field, the objects are simultaneously being attracted to each other.

Using this principle, the magnet works by cementing a piece of a diamagnetic copper in place within an alternating magnetic field. The magnetic field induces eddy currents in the copper, which then produces attractive forces in other diamagnetic materials. However, while the magnet produces attractive forces within the region of the copper, diamagnetic materials will be repelled if placed outside of this region. Thus, the primary limitations of the magnet are that the diamagnetic material attracted needs to be smaller than the surface of the copper region, and the material needs to be placed within the region of magnet's copper plane in order to experience non-repulsive forces.

The construction of the magnet consists of a cylinder with a rod suspended through the center. A copper washer with an inner diameter equal to the diameter of rod and an outer diameter equal to the inner diameter of cylinder is adhered to the face of the magnet. The entire magnet is then wrapped with wire and connected to an alternating voltage source. Passing current through the wires creates a magnetic field B within the core of the magnet described by

$$B = \mu n I_0 \sin(\omega t)$$

where μ is the magnet permeability, n is the number of turns, and $I_0 \sin(\omega t)$ is the alternating current flowing through the coils. This magnetic field passes freely through the outer core of the magnet, while also inducing a current through the copper washer creating a magnetic field in the opposing direction. This effectively creates a shaded pole, in which the flux through the center of the magnet's face lags behind the flux passing through the face of the outer core. Because of this shifting magnetic field, horizontal forces are exerted onto the object towards the center of the magnet's face. Thus, forces are exerted onto the diamagnetic object of interest that attracts the object towards the magnet, while centering the object in the middle of the magnet's face.

The strength of the force produced by the magnet is a function of the eddy currents created in the copper disc in the magnet and the diamagnetic material being attracted. These eddy currents form due to the phenomenon described by Faraday's Law of Induction, in which circular rings of current will be formed around a magnetic field, with a magnitude proportional to the rate of change of the magnetic flux

$$\varepsilon = - \frac{d\Phi}{dt}$$

where ε is the magnitude of the electromotive force and Φ denotes magnetic flux.

From the equation above, it is clear that the strength of the eddy currents can be increased by supplying the coils with more current in order to improve the strength of the magnetic field.

This increases the resistive power loss through the coils, resulting in excessive heating. It is also clear that same effect can be achieved by increasing the rate of change of flux or by increasing the number of windings of the coil. An increased rate of change of flux can be achieved by increasing the frequency of the alternating current with an inverter. Therefore, it can be seen that it is possible to increase the strength of the eddy currents without dramatically increasing resistive loss.

Using this theoretical basis as the framework, and the work performed previously by Leonard Crow, the magnet design was begun. It was agreed early on that an electromagnetics simulator would be needed to verify the viability of different magnet geometries and also to visualize the force acting on the test pieces of metal. From a magnetic circuit viewpoint, the nonferrous magnet is extremely hard to model without some sort of partial differential equations solver. This is because there are flux lines travelling through air for several centimeters, while in a normal magnetic circuit these air gaps would be in the order of a few millimeters. With this in mind, in early January, two different programs were surveyed. The first was Computer Simulations Technology. This program was easy to use. However, this program's free student version was extremely limited, making it unusable for our purposes. We moved on to using ANSYS Maxwell Electromagnetics (Maxwell 3D). The full version was available to us in the lab that we were working in.

Maxwell 3D consists of a CAD environment and a powerful set of numerical solvers that suited the simulation needs. It took us a few weeks to learn how to use it efficiently. We had been simulating the coils of our magnet using helices rather than the coil solver already in the program. This was causing 12-24 hour solver times. Once the coil method was used, we ran multiple tests on the first magnet design that was based on Leonard Crow's original design in rapid succession with the processing time reduced to around ten minutes. The simulations verified that the magnet would be able to attract nonferrous metals.

Our customer also showed interest in designing a magnet using an E core with a shorted secondary. We constructed one for testing and also simulated it. Based on our simulation results, we decided not to devote much time to this geometry. This decision was made because the simulated E core design only started attracting test pieces at frequencies of greater than 1 kHz.

We continued to simulate multiple versions of the Leonard Crow magnet with varying dimensions. Through simulation, we found that the geometry of the design is the key to getting the magnet to actually attract nonferrous metals, along with the strength of the current flowing through the primary wires, as much mentioned previously.

The first magnet that was constructed was the E core design. This magnet did not attract nonferrous metals, but it worked as a normal electromagnet. The first time this magnet was

constructed, 12-gauge AWG wire was used. This design drew so much current that the 15 A fuse in the Variac controlling the AC voltage blew several times. The wire gauge was lowered to 18-gauge and the fuse no longer blew. This was the main reason that 18-gauge wire was selected to be used in the toroidal magnet designs later on. This magnet also dissipated heat rapidly in the ferrite core and the windings. The external temperature was measured after twenty seconds of operation to be greater than 200 degrees C, higher than the rating for the wire or the Kapton tape. The effect of temperature damage to the wiring can be seen in Figure 1 by the darkened wire.

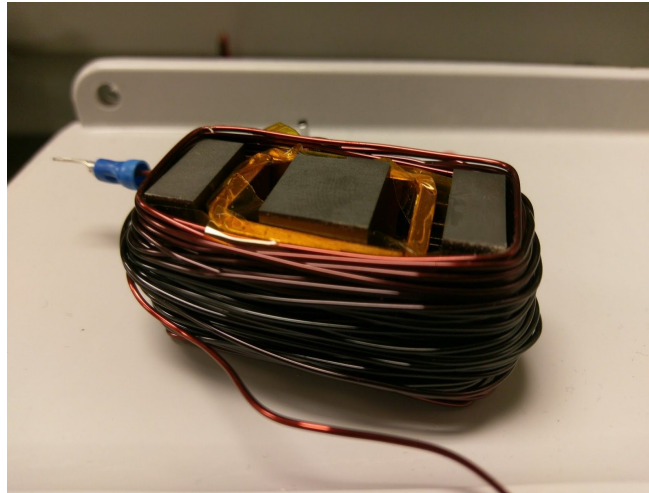


Figure 2. Constructed E core magnet

A copper secondary was constructed both out of 12-gauge wire and a copper bar for testing for use within the E core design. A primary was wound on the outside of the E core consisting of 67 turns of 18-gauge wire. These designs were not successful at attracting any nonferrous metals. This matched the simulated results at 60 Hz which showed no attractive force on a piece of test metal.

The first version of a working nonferrous magnet was based on Leonard Crow's original design. It consisted of a laminated steel outer and inner core, with a shorted copper secondary around the inner core. Around the outer core, the winding of the primary was wrapped. The initial design was powered by 60 Hz alternating current. The following figure shows a mechanical drawing of the first working magnet design:

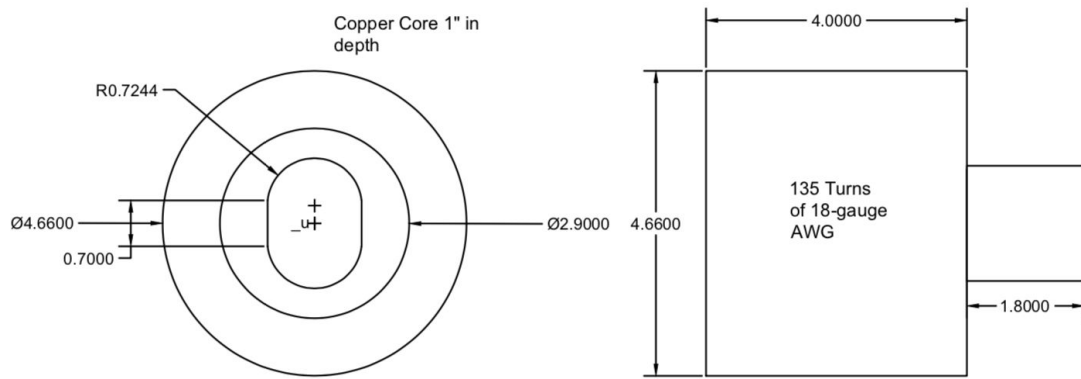


Figure 3. Mechanical drawing of magnet (all dimensions in inches)

Several different types of core materials were analyzed. Powdered iron, ferrite, Mu Metal, and laminated steel. All of these core materials had advantages and disadvantages with regards to geometric availability, saturation, and ohmic heating. For the design, the unique geometry was something that had to be considered, because the availability of the shapes at the dimensions we needed was limited.

We chose to work with laminated steel because it would enable reduced core losses at 60 Hz AC, which was to be the first test frequency, and would work within the range of frequencies that was planned to operate the inverter within, 100-1000 Hz. The dimensional design of the magnet was based on the availability of materials. Laminated steel is not something that comes in a variety of prefabricated shapes. Laminated steel toroids were found on eBay made by a person in New York. The dimensions of the toroids were an inner diameter 2.9", outer diameter 4.66", and height 2". Using this as the basis for the fabrication of the rest of the magnet, we sought to find components to make the copper secondary and the inner core. The cost of these toroids were \$46.60 each.

A scrapped transformer core made of laminated steel was machined down to a circular shape. This machining process was difficult due to the steel laminations, so the core size ended up being an oval with the dimension seen in Figure 2. With the inner and outer core sizes defined, we were able to fabricate the copper secondary.

Three 3 inch by 1 inch copper discs were purchased off of eBay at a cost of \$19.99 each. These discs had to have some of their diameter reduced so that they could fit inside of the inner diameter of the outer core. This left discs with a diameter of 2.9", matching that of the inside diameter of the outer core. One of these discs was machined further, removing the center so that it could be placed around the inner core. The other disc was left solid. This was done to test the necessity of the inner

core. It had been theorized early on that this core worked only as a centering device, which Crow had mentioned only vaguely in his paper, and was not necessary to attract test pieces. It was verified that the center core was not necessary to attract metals in Maxwell 3D before making this decision.

The machining process of the copper was labor intensive. This took almost five hours of machining time. This was due to the necessity to go slow with the milling and lathing processes to prevent the cutters from overheating and being damaged. The copper disc that had to be bored out in the center had to be slowly machined, and it got hot enough to change color in the process.

Two toroids were stacked on top of each other and taped together using Kapton tape. Kapton tape is high temperature tape which is tested by DuPont up to 200 degrees C. Ohmic heating in the core and winding was expected beyond what normal electrical tape could withstand. It was found out later that the core did not heat as quickly as the wires. Most of the thermal issues during the magnet's operation arose from the ohmic losses in the wire. The wires were rated at 200 degrees C. Therefore, thermal protection was integrated into the sensor network in spring with a temperature cut off of 190 degrees C.

The primary was wound by hand around the toroids. For the first magnet, 18-gauge AWG wire was chosen and 135 turns were spun. As mentioned previously, it had been found during experiments with an E core design that higher gauge wire allowed the magnet to draw too much current and blew the fuse in the Variac that we were using, while 18-gauge did not. 18-gauge wire provides a current capacity of 16 A at 90°C.

This magnet was first tested using 60 Hz. It was successful in attracting copper and aluminum, both with and without the inner core. The testing of the first toroidal magnet when connected to 60 Hz AC was successful. We were able to attract copper and aluminum pieces when the voltage was around 45 VAC and 19 A. However, this did cause some damage to the wire of the magnet. We found that the attractive force increased as the voltage and current increased. This verified our simulated research tying attractive force to current through the primary. The highest voltage that was tested was 115 VAC. However, the wire of the magnet got extremely hot, up to 190°C after 30 seconds of operation. The laminated steel cores would reach temperatures of approximately 80°C and the copper secondary around 50°C. Using this information, we determined that thermal protection was a primary concern for the development of this magnet as a piece of industrial equipment.

While the metal test pieces were successfully attracted, they did not hold to the magnet without the support of strings being held by the experimenter. They would begin to slide down the face of the magnet. This meant the attractive force of the magnet was not greater than the force of

gravity that was working orthogonally on the magnet. This method also did not allow us to change the magnetic field frequency since we were using the nominal AC voltage supplied by the building.

Inverter Design and Construction

It was known that the key to making this magnet able to differentiate between metals was the frequency of the magnetic field. This meant that the frequency of the current flowing through the primary coils had to be controlled. In the fall, the use of an inverter was proposed, and an H-bridge topology had been chosen due to its reliability and ease of construction. An H-bridge power inverter using sine-triangular PWM modulation was constructed to enable us to vary the frequency of the magnetic field. This enabled the inverter's output to be a sinusoidally varying signal, which could be used to drive the magnet. For switching devices, we selected the Infineon FF150R12ME3G IGBTs. These were available to us in the lab and at a cost \$92.57 each. There were also evaluation boards that were used as the gate drivers for these IGBTs, simplifying the task of having to construct the gate driver from scratch. The boards were Power Concepts 2SP0115T2A. These cost \$90.05.

An H-Bridge inverter is also referred to as a single phase voltage source inverter. In an H-Bridge, four switches are used. Two switches have high inputs while two have low inputs. As the switches are alternated between on and off, square wave PWM is generated.

However, a square wave PWM would not give the constantly changing current needed for the magnetic field to alternate in the manner needed for the magnet to operate. To overcome this problem, sinusoidal pulse width modulation (SPWM). SPWM involves comparing a triangle wave, the carrier signal, to a sinusoid which has a fundamental frequency equal to the desired frequency of the output voltage.

These IGBTs have a current rating of 200 A and maximum switching frequency of 20 kHz. To implement the sine-triangle modulation, a TI-2833 Delfino Microcontroller DSP was selected. This was attached to a Piccolo experimenter board, part name TMDSDOCK28335, at a total cost of \$154.26. This was selected because a coworker, Atif Maqsood, in our lab, has experience using these DSPs. He assisted in showing how to set up the control system using Simulink, and also in constructing and debugging the inverter.

The DSP was programmed graphically using Simulink. This allows programming with blocks instead of writing C code from scratch. This enables us to change the fundamental frequency within the program. It was originally set to 250 Hz. In the spring quarter, a potentiometer was added to an A/D pin to be able to vary the frequency without having to reprogram the DSP in

Simulink. This was also linked to the control of the overall system. This can be seen in the Appendix Image I.

The original inverter was fed from a 1 kV, 30 A DC power supply through a 450 V, 2200 μ F capacitor to filter stray inductance from the power supply. In the spring this capacitor was increased to 1000 V at 970 μ F. The current then enters the two IGBT packages, mounted on heat sinks, which each contain two IGBTs. These are controlled by the DSP via the gate driver. The outputs of the IGBTs are then connected to the primary of the magnet. The following image shows the first experimental setup for the inverter:

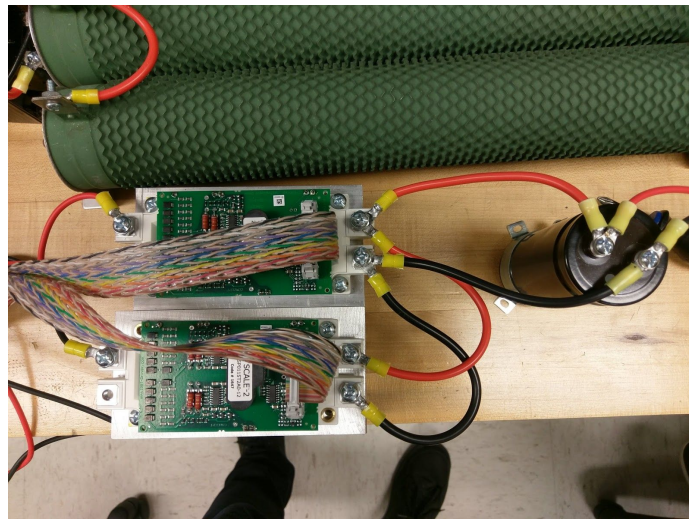


Figure 4. Experimental inverter setup in March of 2018.

After the inverter was constructed, the first iteration of Crow's magnet was connected to it. It was first tested with the DC supply set to 200 V and 5 A, with the inverter set to a frequency of 250 Hz. The magnet performed better than it did powered by 60 Hz, at least in terms of attraction, but the power consumption was still around 1 kW. The attractive force was strong enough that the lighter aluminum piece was able to stick to the magnet without the aid of the experimenter, however, the heavier copper piece did not. This had not been the case using 60 Hz. At 60 Hz, there was an attractive force but it was not enough to keep this piece of aluminum on the magnet. This can be seen in the following figure:

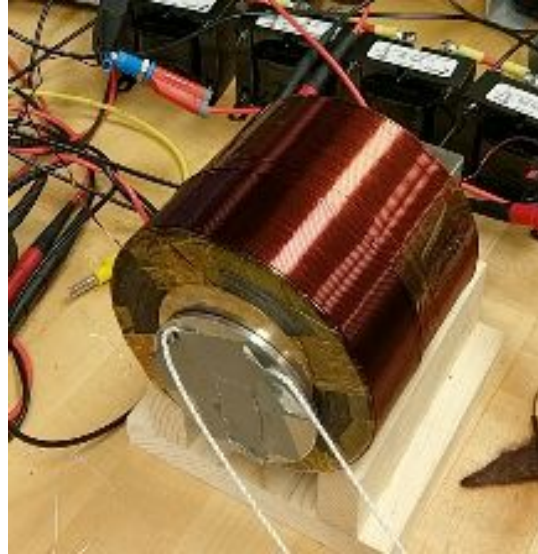


Figure 5. Aluminum disc being held to the 135 turn magnet controlled by the inverter.

It was found that the inverter could not accept a voltage higher than 300 volts. We discussed this with the Ph.D. student who advised us with the design of the inverter. He said that the gate drivers had an automatic shutdown that occurred whenever stray inductances grew to levels that could cause damage to the circuitry. He suggested several remedies, such as placing more capacitors on the inputs of the IGBT, using a busbar to connect the IGBTs instead of wire, or moving the 2200 μF capacitor as close as possible to the gate drivers themselves.

The filter capacitor at the input was replaced by a Cornell Dubilier Electronics 947C971K102DLHS. This capacitor was a metal film capacitor with a capacitance of 970 μF and a DC voltage rating of 1000 volts, which would allow us to maximize the 1 kV power supply in the lab. It was large, measuring approximately 6.5" in height by 4.5" in diameter. It cost \$138.40.

The casing for the inverter was selected to be an aluminum case that was designed to fit into a 19" server rack. This case gave us plenty of space to work with and proper ventilation for the inverters. This cost \$133.70 and was a Bud Industries RM-14213 and associated fixtures. A PCB was designed that powered the gate drivers of the IGBT which needed 15 V, supplied 5 V to the DSP, and jumped the signals from the DSP to the gate drivers. Figure 6, seen below, shows the inverter inside of its enclosure:

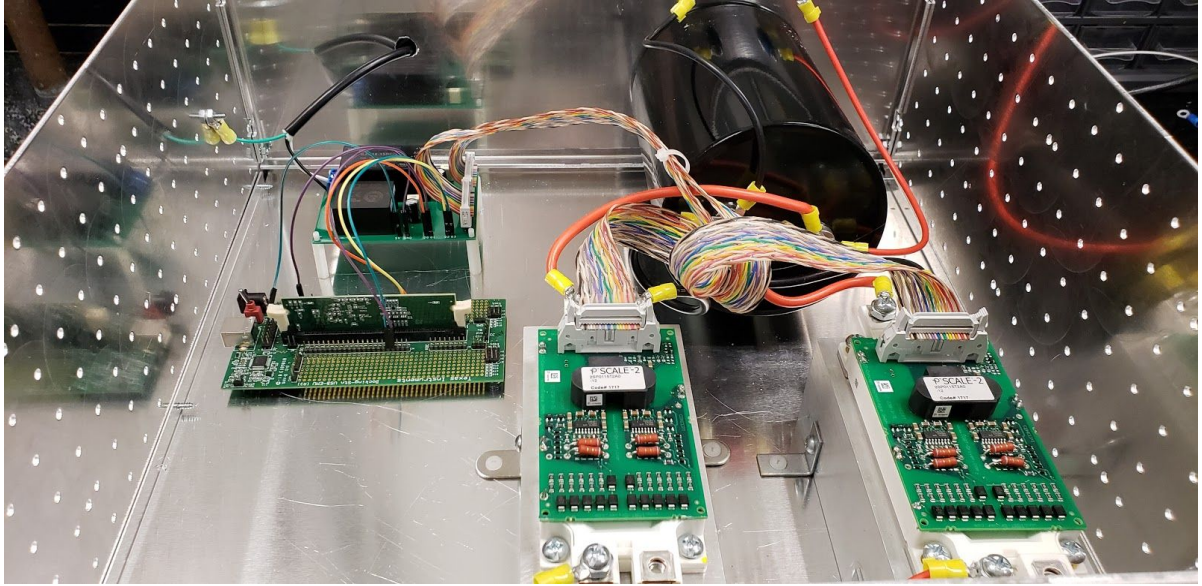


Figure 6. The enclosed inverter

The PCB converted 120 VAC to 15 VDC to power the gate drivers and 5 VDC to power the DSP. The box was grounded for safety. Banana jacks were used for the input and the output of the inverter to ensure safe and reliable connections from the DC supply and to the capacitor bank. 12 AWG wire was used for the connections inside of the H-bridge to ensure the wires would not be damaged by the flow of current which could be up to 20 A based on the inverter design. The IGBTs themselves were mounted on finned, aluminum heat seats to help dissipate heat and prevent damage to them.

The set of tests using the 135-turn magnet and the inverter proved what was expected theoretically. As the frequency of the alternating magnetic field increased, it was expected that the eddy currents being generated in the test metal would increase, and therefore the attractive force would increase, but less current would have to flow through the primary. This means that using a well-designed inverter as a means of increasing the force is essential to making this a commercially deployable system.

Second Magnet Construction and Power Factor Correction

With the experimental success of the first design using both 60 Hz and 250 Hz, a second magnet was constructed using the same dimensions. This magnet was to have an increased amount of turns on the primary in hopes that this would reduce the power consumption of the magnet. This second magnet had 778 turns in the primary winding. It was expected that this second magnet

would have increased forces of attraction in addition to the reduced power consumption that was previously mentioned.

Some sort of enclosure for the magnet itself had to be designed. It had been tested throughout both quarters on a wooden stand with no proper cooling. We purchased a 120V, 6" fan to cool the magnet. The original plan was to suspend it in a steel pipe using plumber's tape. This idea was eventually dismissed due to concerns that the steel would interfere with the magnetic properties of the nonferrous magnet. Upon further discussion with the machine shop operator in Jack Baskin, we decided that an ABS tube, 12" in diameter, with aluminum rods used to suspend the magnet, would be the best method of enclosing the magnet. This enclosure was not fabricated. Due to Magnet-2 being used as a testbed, it was determined that easy access to the magnet was needed by anyone performing tests on it. The fan was attached to the rear of the magnet to provide cooling, but the magnet itself remained in open air. Any magnet of this type going into an industrial facility would have to be enclosed in a properly constructed enclosure that met NEMA and NEC standards. This task in itself would require extensive design. Therefore, it was determined that the vertical and horizontal stands that had already been constructed for the magnet, along with the fan being attached, will be sufficient for any testing performed on the magnet in the future.

The second prototype of 778 turns was tested with the inverter and 60 Hz supply. It was observed that at 60 Hz the magnet worked better than with the 250 Hz inverter supply. This was due to an approximately 3221% increase of inductance as a result of the increased amount of turns around the magnet. With larger inductance, the magnet's impedance was now $77\ \Omega$, and was barely drawing 50 mA of current. The inductance would continue to increase with frequency, thus the reason why the 60 Hz supply worked better with the second magnet than the inverter supply set to 250 Hz.

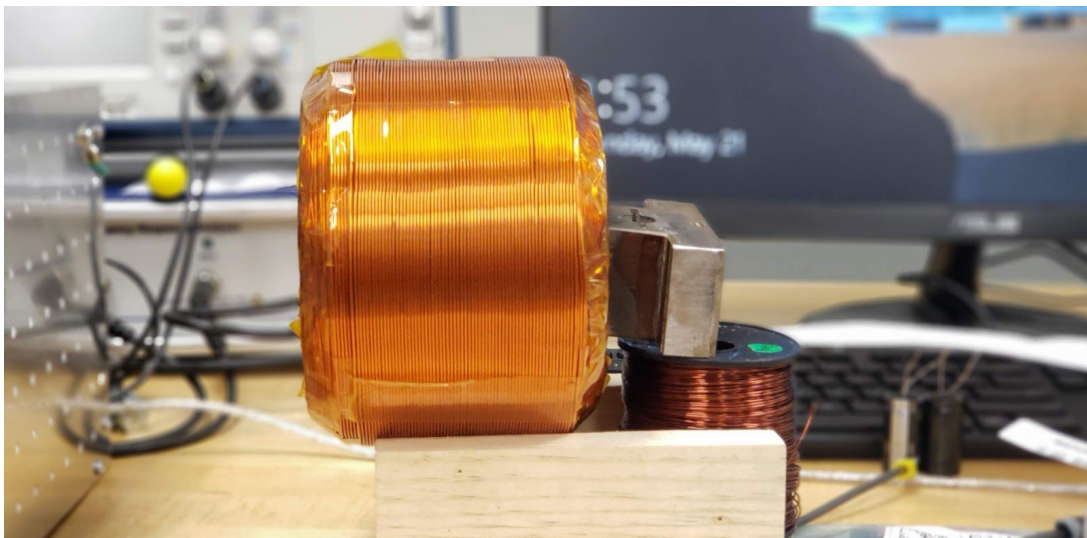


Figure 7. The 778 turn magnet.

The increase in frequency and turns resulted in an increased impedance looking into the magnet. The impedance of the magnet can be described as

$$Z = \sqrt{R^2 + (2\pi fL)^2}$$

where R is the resistance of the wire, f is the frequency of the alternating current, and L is the inductance of the magnet.

An equation of describing the inductance of the magnet can be shown to be roughly approximated as

$$L = \mu_0 \mu_r n^2 I A$$

where μ_r is the relative permeability of the materials within the coils, n is the number of turns per length, A is the area of the face of the magnet, and I is the current passing through the coils.

Thus, it can be seen that the addition of more turns resulted in a small linear increase in resistance and a large quadratic increase in inductance. Increasing frequency also created a linear increase of inductive reactance, which only made the effects of the parasitic inductance stronger. This increased impedance reduced the amount of current flowing through the wires at a given voltage, decreasing the strength of the magnetic field, and thus the attraction force of the magnet. To account for this increase in inductive reactance, capacitance would have to be added in series with the magnet in order to improve the power factor of the system. This is referred to as power factor correction. The impedance of the system, including the parasitic resistance and inductance, with the addition of series capacitors, can be described as

$$Z = \sqrt{R^2 + (2\pi fL - \frac{1}{2\pi fC})^2}$$

where C is the value of series capacitance. From this equation, it can be seen that adding a capacitance with an impedance equal to that of the impedance of the parasitic inductance will result in an impedance equal to only the resistance of the wire. This in term will increase the power factor closer to unity, allowing for more current to flow through the coils and improve the strength of the magnet.

The strength of the nonferrous magnet was improved by increasing the voltage applied across the coils, increasing the amount of turns in the coil, and increasing the frequency of the current, as long as a proper capacitance was implemented in order to compensate for parasitic inductance.

Upon our return from spring break, the paramount task was to develop power factor correction for the 778 turn magnet, which will henceforth be referred to as “Magnet-2” for simplicity. Power factor correction calculations had been performed late in the winter quarter but these had not yet been tested. This was good, because they were “back of envelope” calculations that ended up being wrong and were analyzed again. Upon the recalculation of the power factor for Magnet-2 connected to 60 Hz, it was found that capacitance of 50 μF was needed to offset the inductance. There were 100 μF metal film capacitors rated at 250 V in the lab. Two of these were arranged in series with each other and the with Magnet-2.

This setup was connected to the Variac and the system was test. It was found that this system was successful in drawing around 5 A of current at its maximum voltage. At this current level, Magnet-2 was able to successfully attract both the aluminum and copper disc. It was able to hold the aluminum disc but the heavier copper disc was not able to remain on the face of the magnet.

It was then decided to experiment with a higher voltage. Magnet-2 was connected to a single phase of a three-phase outlet. This enabled it to have a maximum voltage of 208 V at 60 Hz. At this voltage, it drew 10.8 A, and both the aluminum disc and the copper disc were firmly affixed to the attractive face of the magnet. The power consumption was approximately 2.2 kW.

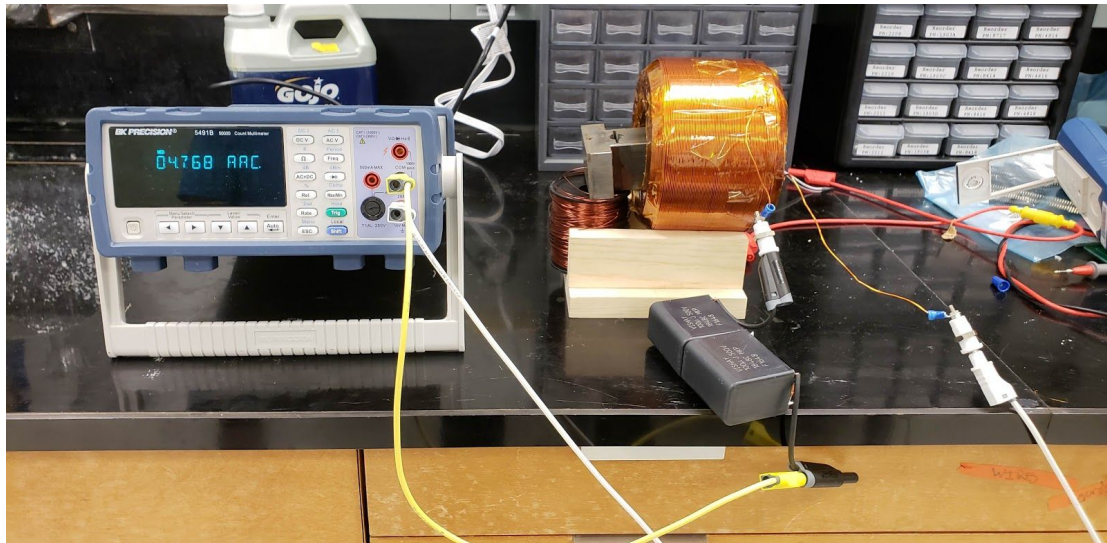


Figure 8. Experimental setup for 60 Hz power factor correction

Having proved that power factor correction would work, metal film capacitors were purchased valued at 1 μF and rated at 600 VAC so that power factor correction could be tested with the inverter set at 250 Hz. These cost \$6.70 each. The needed capacitance had been calculated to be 2 μF . Upon the first test, the current was successfully increased from to 1.90 A at 550 VDC as

measured at the input to the inverter. The aluminum and copper discs were both attracted, however, neither of them stuck to the face of the magnet. Another issue in this experiment was the low rating of the capacitor's voltage. As the voltage was increased from 550 V to 590 V, the impedance was no longer linear. While the current had been 1.9 A at 550 V, it only increased to 1.92 A at 590 volts. We therefore determined that we needed to increase our capacitor rating.

This was not the only cause. We had been relying on the measurements at the input of the inverter, not the measurements at the output, which were alternating currents at a non-rated frequency. Once this was realized, we began to take our measurements at the output of the inverter using the differential voltage probe and the current probe on the oscilloscope. Some 1 uF metal film capacitors rated at 1.5 kVAC at 60 Hz at a cost of \$7.20 each were purchased. Since the test range for the inverter is between 150 and 1000 Hz, it was determined that the parasitic effects seen at high frequencies would not have much effect on our capacitor and these capacitors would work.

These new capacitors enabled the test voltage to go up to 750 volts at the highest test point, but two-in parallel were not giving the expected power factor correction. It was then decided to wire a third capacitor in parallel to see if that would allow more current to be drawn and attain a stronger attractive force. This was done purely as an experimental test, since the theory and calculations told us that the original 2 uF value was accurate. This experiment was successful. The magnet was now able to draw almost 4 amps at 600 VDC, which enabled it to attract and stick both the copper and aluminum discs. The test at 600 VDC is the most important voltage test to perform, since 600 VDC is a common industrial process voltage, along with 480 VAC, three-phase.

The process of power factor correction had not been expected, even though in retrospect it should have been a consideration. Since the end of quarter goal was to have a functional testbed where the frequency could be swept easily, some methods had to be developed to change the power factor correction as the frequency was swept. It was decided that some sort of capacitor bank would be required, which could then be controlled by the sensor network microprocessor as the frequency was changed on the DSP.

Since the impedance of the magnet is proportional to frequency, while the impedance of the capacitance is inversely proportional to frequency, the power factor will not remain constant as frequency is swept. It was necessary to be able to create a means of providing a large variety of capacitance values. This was done by creating a switching capacitor bank which is capable of adding capacitors in series or parallel in order to increase or decrease the value of series capacitance. The equation describing the capacitance, assuming all capacitance values are equal is

$$C_{eq} = \frac{CP}{C^2PS + 1}$$

where P is the number of capacitors in parallel and S is the number of capacitors in series. This capacitor bank topology allowed us to create changes in capacitance by altering the amount of capacitors in series while obtaining a variety of capacitance values in between each series value change by sweeping the value of parallel capacitors. Therefore, we were able to obtain a wide range of capacitance values allowing us to approximate the capacitive reactance to that of the inductance reactance. Knowing the frequency range of interest allows the operator of the magnet to choose a capacitance value and number and series and parallel capacitors in order to achieve a proper minimum and maximum frequency range with acceptable frequency resolution. Six capacitors in parallel and seven in series resulted in 42 different capacitance values. With this, a frequency range of 150 Hz to 1000 Hz was obtained, with an average resolution of 18 Hz between each iteration of capacitance value.

Sensor Network and Capacitor Bank Control

At the same time the capacitor bank was being developed, the sensor network was also being developed. Voltage and current sensors were selected to be at the input and output of the inverter to track the inverters performance. Current and voltage sensors at the output of the capacitor bank, directly before the magnet, were also installed. Along with voltage and current sensors, it was also known that the magnet needed over-temperature protection to prevent the magnet coils from exceeding 200 degrees celsius, their maximum rating. A microcontroller would be used to kill the power when the temperature exceeded 190 degrees C.

We had to decide on a microcontroller to control the sensor network and the capacitor bank. We ended up selecting the Arduino Mega 2560 as our microcontroller because there were several readily available in the lab to begin development of code and testing sensors. They are also simple to use and have developed libraries which would enable us to develop the sensor network and capacitor bank control efficiently. The Mega was used because we needed at least twelve digital pins to control the switching network of the capacitors and we wanted 25+ pins to work with. In an industrial setting, the control of the sensors and actuators would actually be performed by a programmable logic controller. With our testbed, the Arduino Mega was sufficient. These were available for \$38.50.

Once the microcontroller had been selected, characterising the sensor networks was the next step. The voltage sensor was selected to be the LEM LV 20-P due to its accuracy, good linearity, low thermal drift, low response time, high bandwidth, and high immunity to external interference. These cost \$45.54. The current sensor was chosen to be the LEM LA 55-P, a Hall effect sensor, which was selected because of its accuracy, linearity, low temperature drift, response time, immunity to

external, interference, and current overload capability. These cost \$26.54. We debated between using thermistors, thermocouples, and resistive thermal devices as an over-temp sensor. We ended up choosing a thermocouple, but this would give us some issues later on. These cost \$25.69 for the thermocouple and \$10.79 for the MAX6675 thermocouple amplifier board.

To implement the LEM LV 20-P voltage sensor, we needed ± 12 V power rails, which we obtained by using a RAC10-12DK/277 board mount power supply, which cost \$11.87. This voltage transducer requires a 10 mA current passing through the device from the voltage source being measured. A resistance had to be placed in series with the sensor's input and the voltage we wanted to measure. We decided that the average voltage supplied to the magnet was around 500 V, thus we choose a resistance of $50\text{ k}\Omega$. The power delivered to the resistance was found to be 5 W. We then sourced a $50\text{ k}\Omega$ resistance with the proper power rating to fulfill the 10 mA input current requirement. The voltage transducer has an output current mirror with a current related to the measured voltage by a scaling factor. This current was measured over a $100\text{ }\Omega$ resistor and the scaling factor was found by measuring the output current and comparing it to a known voltage input, where the scaling factor was then found to be $k = V_{Known}/V_{100\Omega}$. Through code, the measured voltage value was found by $V_{Meas} = k * V_{100\Omega}$.

To implement the LEM LA 55-P current transducer, it was supplied with ± 12 V power rails from the same power supply used for the voltage sensors. The current sensors need 50 A passing through them for best accuracy, so loops of wires were threaded through them until a value close to 50 A was made. The number of loops is equal to the nearest integer value of $50\text{A}/I_{Measure}$. The output of the current sensor is also a current mirror with a current related to the current being measured by a scaling factor. To measure this output current, we measured the voltage over a $100\text{ }\Omega$ resistance that we placed on the output of the sensor. The current being measured was then found by multiplying the output current by the conversion ratio of 1:2000. Thus, the measured current was found by $I_{Meas} = 2000(V_{100\Omega}/100\Omega)$.

It had been decided to use a thermocouple due to their wide temperature sensing range and linearity. However, an issue arose when we placed the sensor near the operating magnet. The large alternating electromagnetic field interfered with the inductance of the wire, and created large voltage spikes on the signal. Efforts were made to remove this noise with analog low pass filters, however we could not create one that was effective enough to remove the large spikes entirely. We found it was better to filter this noise digitally, by writing a program that would recognise and discard improbable voltage readings to remove the obvious voltage spikes. Then only the approved data was passed through a moving average filter. However, the thermocouple is only capable of taking readings once every 200 ms, limiting us to a sample size of 5 per every second resulting in a

particularly slow data output. Looking back, using an thermistor would likely have been a better choice, for we could have increased the ADC sample rate to around 9.6 kHz, resulting in a faster means of removing the noise. However, the rate at which the temperature of the magnet rises is slow enough, that our current sample rate with the thermocouple was deemed acceptable for our use.

The final step was integrating the control system. Originally it was thought we could use SCRs to control the switching for the capacitor bank, but we realized that we would not be able to reset them when we needed to. It was decided to use relays. We ended up selecting a TE Connectivity Potter & Brumfield Relays rated at 40 A controlled by 12 volts which cost \$2.83 each. MOSFETs were selected to drive the contacters of the relays. We decided to use RFP30No6LEs, which were \$1.69 each. These MOSFETs are rated for 30 A with an on resistance of $47\text{ m}\Omega$. Thus, the MOSFETs would be able to easily handle the 130 mA needed to activate the relays with little risk of them overheating or being affected by any inductive kicks while switching the relays. To handle the inductive kicks, 1N4001 diodes were used to short the high inductive voltages to the power supply in order to protect the MOSFETs. These were successfully breadboarded and tested before being added to the design of the sensor network PCB.

Once the current and voltage sensors had been characterized and the relay switching had been determined, we were able to combine this whole system along with the Arduino Mega onto one printed circuit board. This board was almost a square foot when it was laid out. It had a total of twenty MOSFET switches for the relays, eight extra, just in case the capacitor bank was expanded in the future. There were three connections each for the voltage sensors and current sensors, and a jumper for the ring encoder which would enable the values of the capacitor bank to be controlled.

Upon receiving the PCB board from EasyEDA at a cost of \$70 for five boards, the board was populated and tested. There were some minor errors that had to be dealt with. The drill holes for the Arduino were for the smaller Arduino, not the Mega, so the Arduino was hot glue gunned to the PCB. Another major issue was the pinout for the positive 12V supply, a Meanwell IRM-45-12 costing \$13.50. Due to the amount of current needed to drive the relay switching, a separate 12 V voltage converter was chosen, separate of the smaller one that powered the negative 12 volts needed for the current sensors. The output pins on the positive 12 volt supply were fed to a 12 volt plane on the PCB, however, the pin connections for the output to this plane had been reversed by the designer. To rectify this situation to enable testing without having to wait for a new board, the power supply brick was placed on standoffs and 18 gauge wire was fed to the proper connections. This successfully solved the error and the various components needing the +12 V, the current and voltage sensors, and the relays, were powered.

Next, the Arduino code was combined which enabled control of the system. The relays were successfully turned on and off using the code after some simple fixes to the original version. The current and voltage sensors, having being properly characterized, were tested and their readings were sent to an LCD display. The frequency was also displayed on the LCD, based on the value of the A/D controller on the DSP in the inverter, along with a coded value that indicated the capacitance of the capacitor bank.

The capacitor bank had to be wired separately from a PCB because of the high currents potentially flowing through the relays. The fabrication of this was a tedious and arduous soldering job using 22 gauge wire for the control signals and 12 gauge wire to the connections to the contacters of the relays and the capacitors. The following image shows the constructed capacitor bank:

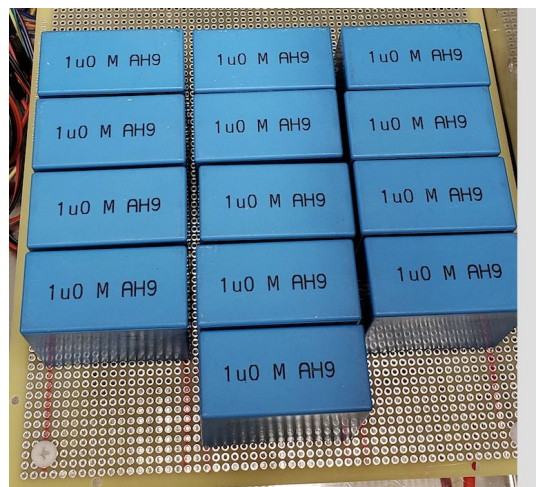


Figure 9. The capacitor bank

The capacitor bank and the sensor network board were put into a 19" server rack box similar to that of the inverter. This gave us plenty of space to work with, which was necessary to the large size of the PCB and the board containing the capacitors and relays. Once again, the case was grounded and banana plugs terminals were used for the external to internal connections. Figure 10, seen below, shows the completed network sensor and control PCB.

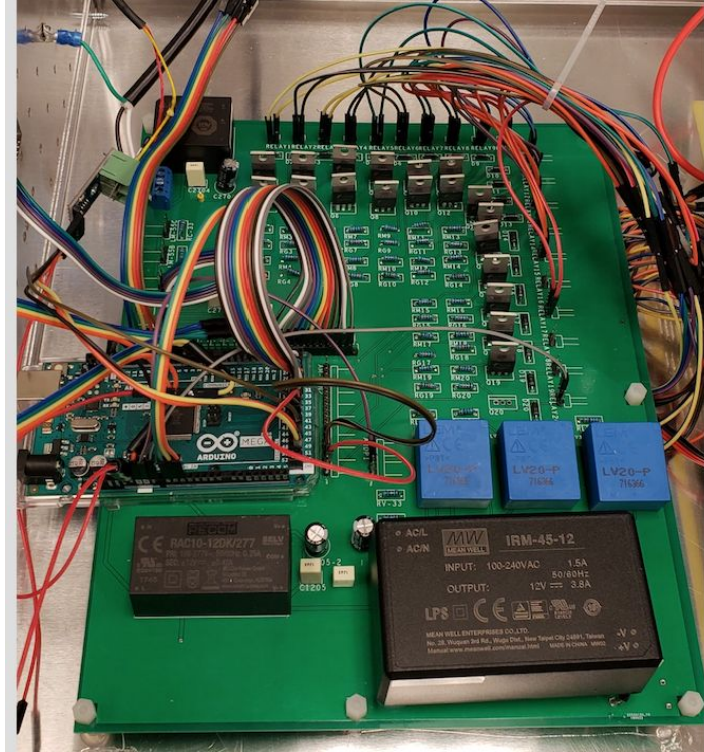


Figure 10. The PCB for the sensor network

Finally, the inverter, the capacitor bank, the sensor network, and the magnet were all integrated together and tested. The capacitor bank still needed to be refined to be able to switch easily as the frequency of the inverter was adjusted.

Conclusion

We are pleased with the work that we have performed during the past six months. We had a goal of four major milestones originally outlined in the introduction: A specialized electromagnet capable of attracting nonferrous metals, an inverter to control the magnetic field frequency, the development of a sensor network to gather data and control the magnet's operation, and the development of code to integrate the systems. We achieved all of the major milestones. However, we had two major stretch goals, the first was to prove that by controlling the frequency of the magnetic field we would be able to differentiate between attracting copper and aluminum, and the second was the writing of a rough draft of a journal paper based on those results. While we are disappointed that we were not able to achieve these stretch goals, we have developed a functioning testbed with which further research can be performed in the future by our customer's research team.

The two deliverables planned for Winter Quarter were a modified electromagnet capable of attracting nonferrous metals using a 60 Hz power supply and an inverter supply which

would allow us to test different frequencies on the electromagnet. Both deliverables were successfully completed and tested. Our customer was satisfied with the results. We also completed all of our tasks that we outlined in our Gantt chart. This included simulating various magnet geometries, fabricating two magnets, and the design and construction of an inverter that can be used to increase the frequency of the magnet. Our customer also asked us to research various different methods of attracting nonferrous metals. This research was unsuccessful.

As we progressed into spring quarter, we ran into a major technical issue that was overlooked in our original design. This forced us to make significant design changes. We had constructed a 778 turn magnet which had an high inductance of 183 mH. This high inductance created a impedance of $77\ \Omega$. Since the ability to attract nonferrous metals was based on the current through the primary coil of the magnet, we had to add power factor correction to reduce the impedance caused by the inductance of the magnet. This power factor correction also had to be able to vary in capacitance as the frequency changed, and therefore an adjustable capacitor bank was constructed simultaneously with the sensor network.

Our overall work in the spring quarter was productive. We were able to create a functioning sensor network and capacitor bank. These were then integrated with the magnet and inverter developed in the winter. We were able to write code to operate the sensor network, the DSP controlling the inverter, and the capacitor bank.

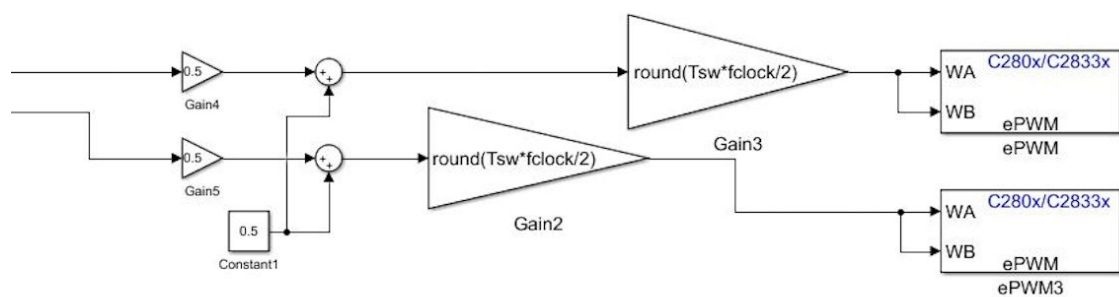
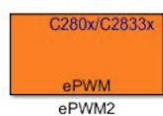
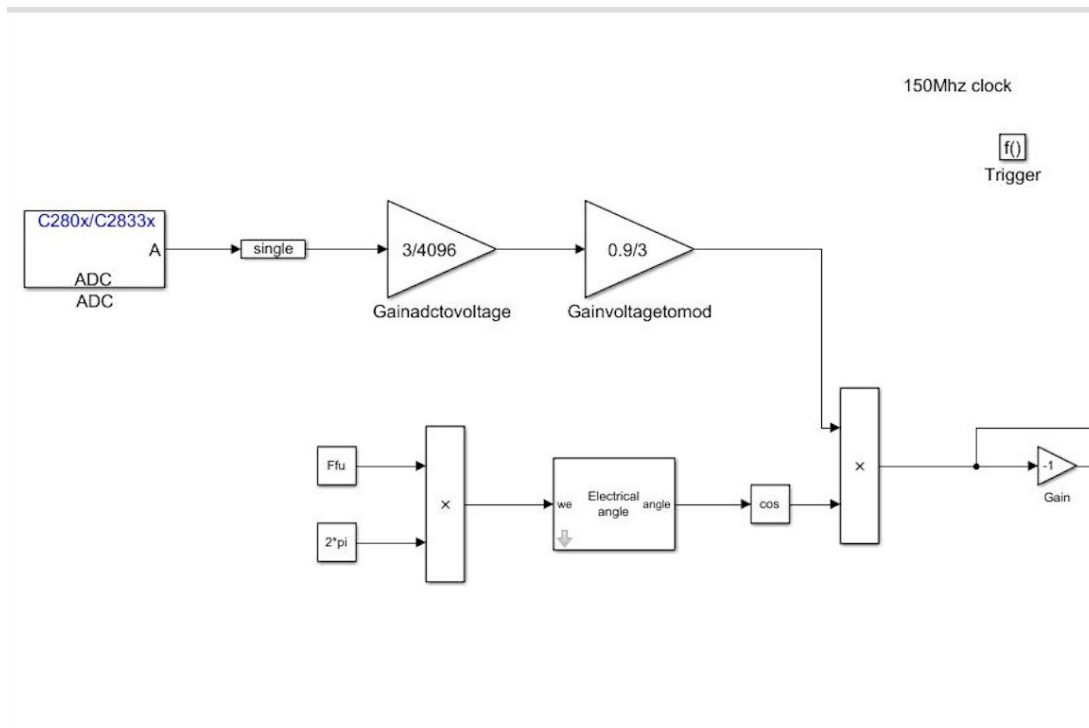
The two major unforeseen issues, power factor correction and over-temp protection were both eventually resolved. The solution to the power factor correction was simple, but it was a time consuming process to design and construct a capacitor bank that would sweep with frequency. Conceptually, the idea is simple, however, implementing it in a useful and simple way required time. The solution to the over-temp protection was also simple, but it required testing and backtracking to finally resolve.

A major result of our experimenting with various voltage levels at various frequencies with both magnets was that the power consumption required to retain the aluminum disc were all very similar. This “retention point”, the point at which the force is strong enough to hold the disc, was 2.2 kW for Magnet-2 at 208 V, 60 Hz, and 1.8 kW for Magnet-2 at 600 VDC, 250 Hz. As mentioned previously, the 600 VDC test is vital because this is a common value for industrial processes. The 208 VAC test is also valuable for the same reason. This means that is an industrial facility using 480 V three-phase power for its processes, three magnets could operate off of one line. However, this would not allow for the magnet to differentiate between different types of nonferrous metals, and therefore would not solve the sorting issue.

The total cost of the testbed was below \$2100. We spent less than \$2800 on our total purchases, not including the necessary lab equipment. These costs do not include the development of proper casing for the magnet. The most expensive component to our system was the inverter because the IGBTs and the gate drivers cost approximately \$700 alone. The magnet's total cost came in under \$400 dollars.

Overall, the major milestones were achieved, but the stretch goal of differentiating between different metals was not. This is the next step in the development of this technology as a method of sorting nonferrous metals. It is our hope that this will be performed next year by another team.

Simulink Inverter Control



References

1. L.R. Crow. *Design, Construction and Operating Principles of Electromagnets for Attracting Copper, Aluminum, and Other Non-Ferrous Materials*. Universal Scientific Company, 1951.
2. Stoll, Richard L. "The analysis of eddy currents." (1974).